

Conformal cosmological black holes: Towards restoring determinism to Einstein theory

Fayçal Hammad^{1,2,3,a}, Dilek K. Çiftçi^{1,4,b}, and Valerio Faraoni^{1,c}

¹ Department of Physics and Astronomy & STAR Research Cluster, Bishop's University, 2600 College Street, Sherbrooke, QC, J1M 1Z7, Canada

² Physics Department, Champlain College-Lennoxville, 2580 College Street, Sherbrooke, QC, J1M 0C8, Canada

³ Département de Physique, Université de Montréal, 2900 Boulevard Édouard-Montpetit, Montréal, —QC, H3T 1J4 Canada

⁴ Department of Physics, Namık Kemal University, Tekirdağ, Turkey

Received: 21 March 2019 / Revised: 15 May 2019

Published online: 2 October 2019

© Società Italiana di Fisica / Springer-Verlag GmbH Germany, part of Springer Nature, 2019

Abstract. A widespread solution-generating technique of general relativity consists of conformally transforming known “seed” solutions. It is shown that these new solutions always solve the field equations of a pathological Brans-Dicke theory. However, when interpreted as effective Einstein equations, those field equations exhibit, in the case of a cosmological “background”, an induced imperfect fluid as an additional effective source besides the original sources of the “seed” solutions. As an application of this feature, the charged non-rotating Thakurta black hole, which is conformal to Reissner-Nordström, is used to demonstrate the fragility of the inner Cauchy horizon when this black hole is embedded in the universe (even accounting for the separation of black hole and Hubble scales). Furthermore, we show that the charged McVittie spacetime, although not conformal to any GR solution, represents a charged black hole embedded in a cosmological “background” with varying Hubble parameter that does not exhibit a real Cauchy horizon. These arguments speak in favor of restoring determinism to Einstein theory, which was questioned in recent research.

1 Introduction

The most general spherically symmetric and asymptotically flat solution of the coupled Einstein-Maxwell equations is the Reissner-Nordström (RN) geometry describing a charged black hole. Excluding the extremal and super-extremal cases, this static solution has a null event horizon (the outermost black hole horizon) which encloses a null Cauchy horizon. Cauchy horizons are surfaces through which the geometry can be continued but cannot be predicted by prescribing regular initial data. In other words, they are null hypersurfaces that constitute the boundary of the domain of validity of the Cauchy problem for spacetime. The existence of such a boundary, avoided only by the strong cosmic censorship conjecture [1], implies the loss of determinism in such a spacetime. Therefore, the initial value problem of vacuum GR fails in the interior of a charged black hole and the theory ceases to be predictive and deterministic, a completely unacceptable shortcoming for any fundamental physical theory or for its solutions. Realistic astrophysical black holes are not charged nor static: they are electrically neutral and they rotate. However, static charged black holes have been used in the recent ref. [2] as toy models for realistic black holes.

Fortunately, there is a long history of indications that the Cauchy horizon inside the RN black hole is an artifact of the perfect symmetries of the latter: it is fragile and it disappears when these symmetries are broken or the RN solution is perturbed. Specifically, photons arriving to the Cauchy horizon from larger radii are infinitely blueshifted (a phenomenon known as *mass inflation*) and a mass inflation singularity develops when this phenomenon is taken into account [3]. The Cauchy horizon is then unstable with respect to perturbations of the RN solution, which decay outside the event horizon but grow in the region inside of it because of the infinite blueshift, transforming the Cauchy horizon into a singularity through which the spacetime cannot be continued.

^a e-mail: fhammad@ubishops.ca

^b e-mail: dkazici@nku.edu.tr

^c e-mail: vfaraoni@ubishops.ca

In ref. [2] (see also ref. [4]) it was pointed out, through a clever study of the quasinormal modes, that adding a positive cosmological constant Λ to the picture, the resulting Reissner-Nordström-de Sitter (RNdS) solution of the Einstein equations exhibits a decay rate of the perturbations outside the black hole horizon which is quite different from that of the RN black hole (exponential instead of power law [2]). Since the decay rate outside the black hole horizon is tied to mass inflation near the Cauchy horizon, the latter is stabilized by the cosmological constant and determinism is again in jeopardy. This fact is worrisome since, ultimately, no black hole is isolated but it is embedded in the universe and the asymptotics are not Minkowskian, but cosmological. Therefore, the RNdS model is a more realistic model of a black hole than a RN one and the introduction of Λ in [2] is well justified. Even though the asymptotics are usually neglected for astrophysical black holes evolving on temporal and spatial scales much smaller than the Hubble radius, this cannot always be done in problems of principle, as ref. [2] shows, because even a tiny cosmological constant can make a profound difference.

The conclusions of ref. [2] have been challenged in refs. [5–8]. In refs. [5–7] it is pointed out that scalar field perturbations around a charged black hole necessarily involve a charged scalar field, and that its decay rate outside the black hole horizon is not altered with respect to the RN case. Reference [8] studies, instead, electrically neutral but rotating black holes in a de Sitter background and shows that the Cauchy horizon is again unstable for this more realistic situation. While the debate continues [9–12], ref. [13] points out persistent evidence of the loss of determinism in a finite region of parameter space. Here we propose an independent approach and we point out a different, non-perturbative way in which the Cauchy horizon is destroyed by modifying the black hole model to make it more realistic. In fact, although the perturbations of the RNdS geometry described by quasinormal modes help break the symmetries, the real universe is not described by an exact de Sitter model. While de Sitter is the late-time attractor of many dark energy models attempting to explain the current acceleration of the universe (including that caused by a cosmological constant) [14], and de Sitter space may ultimately turn out to be its final asymptotic state, the real universe contains dark and ordinary matter, radiation, neutrinos and other forms of mass-energy and is not completely empty. The matter stress-energy tensor T_{ab} in the right-hand side of the Einstein equations with cosmological constant Λ^1 ,

$$G_{ab} \equiv \mathcal{R}_{ab} - \frac{1}{2} g_{ab} \mathcal{R} = 8\pi T_{ab} - \Lambda g_{ab}, \quad (1)$$

cannot be neglected entirely. As a consequence, the cosmological model describing our universe is not a pure de Sitter space, but rather a FLRW one. Then, a better model of a black hole with non-Minkowskian asymptotics is one in which this object is embedded in a non-static FLRW universe. Strictly speaking, though, real black holes exist in the dynamic backgrounds of surrounding matter (stars, star clusters, galaxies, etc.) that create much larger curvatures than the cosmological backgrounds. Therefore, the reader should keep in mind that while the simple picture of a black hole used here is certainly more general and closer to that of realistic black holes in nature than the static ones, this still constitutes only a working toy model.

There are immediately two problems arising with such simplified models, though. First, while the RNdS geometry is the unique spherical, static, and asymptotically de Sitter solution of the coupled Einstein-Maxwell equations, there is no unique solution with dynamical FLRW asymptotics. While a few exact solutions of the Einstein equations (and their charged versions) are known, they are special and they usually suffer from some physical pathology (see ref. [16] for a review). We argue that they are still better models of charged black holes than the RNdS space in the sense that they model the cosmological asymptotics in a general (instead of locally static) way.

The second problem is that, while in stationary situations (such as for the RNdS model) black hole horizons are static and null surfaces, for dynamical black holes one must consider instead *apparent* horizons (AHs), which are dynamical and are spacelike or timelike. However, AHs are foliation-dependent, as exemplified dramatically by the fact that in the Schwarzschild spacetime there exist foliations without AHs [17,18]. This problem is somehow alleviated by the recent realization that, in spherical symmetry, all spherically symmetric foliations (to which we restrict here) possess the same AHs [19]. In any case, the recent detections of gravitational waves from black hole mergers by the LIGO interferometers [20–23] are based in an essential way on the use of marginally trapped surfaces and AHs. In fact, due to the low signal to noise ratio, gravitational wave signals are matched to banks of templates for the gravitational waveforms, which are produced by numerical simulations identifying black holes with their apparent, not event, horizons. Event horizons are essentially useless for this practical task. The new and promising gravitational wave science is based on AHs when these waves are generated by mergers of black holes with other objects.

Keeping in mind the two *caveats* above, one can nevertheless study particular solutions of GR describing charged black holes embedded in FLRW universes as more general toy models than RNdS. We discuss two examples in which, changing the background from static Minkowski or de Sitter to FLRW, the inner Cauchy horizon disappears. This is a further indication that the Cauchy horizon is very fragile and is not expected to occur in nature, helping restore determinism to GR.

Another topic in gravitational physics, that might seem outside the purpose of the present paper, is conformal transformations. Conformal transformations of the spacetime metric play an important role in general relativity (GR)

¹ Throughout this paper, we use units in which Newton's constant G is unity and we use the notations of ref. [15].

in the study of conformal infinity and in the construction of Penrose-Carter diagrams [15], in alternative theories of gravity where different conformal frames (the Jordan and the Einstein frames) provide alternative representations of these theories [16, 24, 25], in highlighting the true nature of some of the quasi-local definitions of mass in GR and in scalar-tensor gravity [26, 27], in examining from a different angle the thermodynamics of black holes [28] and the thermodynamics of classical spacetime in general [29], and in investigating the relation between the energy conditions and wormholes [30]. More important for us, however, is the fact that conformal transformations are also used in GR as a technique to generate new analytic solutions of the Einstein equations starting from known ones, particularly in the case of electrovacuum [31–44], but also in the presence of fluids [45–49]. This technique allows, in fact, to change the background of a given GR solution from the static Minkowski or de Sitter to the needed FLRW. This technique has even more potential in the context of scalar-tensor gravity as it allows to obtain the general vacuum and electrovacuum static, spherically symmetric solutions, including the Brans-Dicke theory as a special case [50]. This technique has subsequently been used [51–58] to generate the general spherically symmetric static solution of vacuum Brans-Dicke theory from a known general solution of GR (see, *e.g.*, [59] and the references therein). For our present purpose of tackling the issue of determinism loss in Einstein’s theory, however, we restrict ourselves to GR.

Let the spacetime metric g_{ab} be a solution of the Einstein equations (1) without the cosmological constant. Then, it is *a priori* possible that the conformally related metric

$$\tilde{g}_{ab} = \Omega^2 g_{ab}, \tag{2}$$

where Ω is a nowhere-vanishing, regular, conformal factor is still a solution of the Einstein equations. In order for this new solution to be of any physical interest, however, the conformal factor Ω must be chosen judiciously. Over the years, there has been increasing interest in generating solutions of the Einstein equations which describe black holes embedded in cosmological “backgrounds”². In these cases, the metric g_{ab} usually describes a black hole (Schwarzschild, Kerr, or their charged generalizations) and the conformal factor Ω is chosen as the scale factor of a spatially flat Friedmann-Lemaître-Robertson-Walker (FLRW) universe, which comes to constitute the cosmological “background”. This procedure has generated the Thakurta [32], Sultana-Dyer [41], McClure-Dyer [42], and other solutions such as spherical perfect fluid solutions [45–49].

The new metric \tilde{g}_{ab} is not a solution of the Einstein equations with the same form of matter source for which the original metric g_{ab} is a solution, though. In fact, under the conformal transformation (2), the Ricci tensor changes according to [60]

$$\tilde{\mathcal{R}}_{ab} = \mathcal{R}_{ab} + \frac{4\nabla_a\Omega\nabla_b\Omega}{\Omega^2} - \frac{2\nabla_a\nabla_b\Omega}{\Omega} - g_{ab} \left[\frac{\square\Omega}{\Omega} + \frac{\nabla_e\Omega\nabla^e\Omega}{\Omega^2} \right], \tag{3}$$

while the trace of this equation gives

$$\tilde{\mathcal{R}} = \Omega^{-2} \left(\mathcal{R} - \frac{6\square\Omega}{\Omega} \right), \tag{4}$$

so that eq. (1) becomes

$$\begin{aligned} \tilde{G}_{ab} &= \kappa T_{ab} - \frac{2}{\Omega} (\nabla_a\nabla_b\Omega - g_{ab}\square\Omega) + \frac{1}{\Omega^2} (4\nabla_a\Omega\nabla_b\Omega - g_{ab}\nabla_c\Omega\nabla^c\Omega) \\ &\equiv \kappa \left(T_{ab} + T_{ab}^{(\Omega)} \right). \end{aligned} \tag{5}$$

Thus, a vacuum solution g_{ab} (with $\mathcal{R}_{ab} = 0$) is transformed into a non-vacuum one with $\tilde{\mathcal{R}}_{ab} \neq 0$. The derivatives of the scale factor Ω act as an effective form of matter in the right-hand side of the Einstein equations. Since generating new solutions in this way amounts to the “Synge procedure” of imposing the form of the metric and then running the Einstein equations to determine the matter that makes the chosen metric a solution, there is *a priori* little hope that this artificially created effective matter $T_{ab}^{(\Omega)}$ will be physically meaningful. Indeed, the right-hand side of the tilded Einstein equations (5) contains, in addition to “standard” terms quadratic in the gradient $\nabla_a\Omega$, terms linear in the second derivatives $\nabla_a\nabla_b\Omega$ and $\square\Omega$. These terms make the sign of the effective energy density undefined and $T_{ab}^{(\Omega)}$ will not, in general, satisfy any energy condition. In fact, the “cosmological black hole” geometries generated this way are often reported to exhibit negative energy densities in certain spacetime regions [41, 42]. Furthermore, the new solutions thus obtained might actually exhibit singularities that may or may not be present in the original solution. Indeed, as can be seen from (4), the new Ricci scalar $\tilde{\mathcal{R}}$ might possess a singularity whenever the inverse metric component in $\square\Omega = g^{ab}\nabla_a\nabla_b\Omega$ becomes singular.

Nevertheless, these solutions of GR are still seen as interesting at least as toy models of black holes, and they are put to use, for example, in recent investigations of the Hawking radiation and thermodynamics of dynamical black

² We use quotation marks because, due to the non-linearity of the field equations, one cannot split a metric into a “background” and a “deviation” from it in a covariant way (apart from algebraically special geometries, such as the Kerr-Schild ones).

holes (see [61,62,64–67] also the related refs. [68–70]). Furthermore, the Husain-Martinez-Nuñez solution of GR [39] is conformal to the Fisher solution (with the scale factor of the FLRW “background” universe as the conformal factor), but has as the matter source a canonical, minimally coupled, free scalar field which satisfies both the weak and null energy conditions. The same can be said about its generalization in which the scalar acquires an exponential potential, known as the Fonarev solution [40]. It may even happen that an unphysical solution of the Einstein equations is conformally transformed into a physically interesting one, as is the case for the fluid spheres of ref. [45]. On the other hand, whenever g_{ab} is an (electro)vacuum solution of the Einstein equations, the geometry $\tilde{g}_{ab} = \Omega^2 g_{ab}$ can always be seen as a solution of a Brans-Dicke theory with Brans-Dicke coupling $\omega = -3/2$. This theory is known to be pathological³, in the sense that the Brans-Dicke field $\phi = \Omega^{-2}$ is non-dynamical and, more important for us, the Cauchy problem becomes ill-posed. The pathology is then just a reflection of the fact that the conformal factor Ω is forced arbitrarily into the geometry by imposing that \tilde{g}_{ab} describe a central object in a cosmological “background”, and this fact is obviously bound to have consequences.

The outline of the rest of this paper is as follows. Section 2 discusses these general aspects of obtaining new solutions of the Einstein equations via conformal transformations; sect. 3 discusses an ambiguity present in the literature about the non-rotating Thakurta and Sultana-Dyer cosmological black hole geometries, which are of the kind described above. The following section focuses on the non-rotating Thakurta solution, which is of special interest in both GR and scalar-tensor gravity. We use this conformally created solution there as a counterexample to study the (absence of the) inner Cauchy horizon in cosmological black holes. Section 5 proposes yet another cosmological black hole which cannot be built by a conformal transformation, as a useful example in the debate about inner Cauchy horizons in GR black holes. Finally, sect. 6 contains the conclusions.

2 GR seed geometries and $\omega = -3/2$ Brans-Dicke gravity

In this section we expose the physical features we gain by using conformal transformations to construct a new solution from a given GR solution. In addition, we also describe the status of such a process within the framework of Brans-Dicke theory.

Assume that g_{ab} is an (electro)vacuum solution of the Einstein equations (1) obtained from the Einstein-Hilbert action

$$S = \int d^4x \sqrt{-g} \left[\frac{1}{2\kappa} (\mathcal{R} - \Lambda) + \mathcal{L}_{(m)} [g_{ab}, \psi] \right], \tag{6}$$

where Λ is the cosmological constant and $\mathcal{L}_{(m)} [g_{ab}, \psi]$ is the matter Lagrangian, with ψ denoting collectively the matter fields. Consider the conformal metric $\tilde{g}_{ab} = \Omega^2 g_{ab}$: by using eqs. (3), (4), and

$$\sqrt{-\tilde{g}} = \Omega^4 \sqrt{-g}, \quad \frac{\square \Omega}{\Omega^3} = \frac{\tilde{\square} \Omega}{\Omega} - \frac{2\tilde{g}^{ab} \tilde{\nabla}_a \Omega \tilde{\nabla}_b \Omega}{\Omega^2}, \tag{7}$$

and introducing the scalar field $\phi = \Omega^{-2}$ (which will become a Brans-Dicke scalar), one easily obtains

$$\sqrt{-g} \mathcal{R} = \sqrt{-\tilde{g}} \left(\phi \tilde{\mathcal{R}} + \frac{3}{2\phi} \tilde{g}^{ab} \tilde{\nabla}_a \phi \tilde{\nabla}_b \phi \right) - 3\partial_c \left(\sqrt{-\tilde{g}} \tilde{g}^{ac} \partial_a \phi \right). \tag{8}$$

In terms of \tilde{g}_{ab} and ϕ , the Einstein-Hilbert action (6) becomes

$$S = \int d^4x \sqrt{-\tilde{g}} \left\{ \frac{1}{2\kappa} \left[\phi \tilde{\mathcal{R}} + \frac{3}{2\phi} \tilde{g}^{ab} \tilde{\nabla}_a \phi \tilde{\nabla}_b \phi - V(\phi) \right] + \tilde{\mathcal{L}}_{(m)} [\tilde{g}_{ab}, \psi] \right\}, \tag{9}$$

where the total divergence in the right-hand side of eq. (8) (which only contributes a boundary term to the action), has been dropped, the cosmological constant has become the mass potential

$$V(\phi) = \frac{\Lambda}{2\kappa} \phi^2 \equiv \frac{\mu^2 \phi^2}{2}, \tag{10}$$

and the matter Lagrangian density reads now $\sqrt{-\tilde{g}} \tilde{\mathcal{L}}_{(m)} = \phi^{-2} \sqrt{-g} \mathcal{L}_{(m)} [\phi \tilde{g}_{ab}, \psi]$. This is a (Jordan frame) Brans-Dicke action [78] with coupling parameter $\omega = -3/2$. Its variation with respect to \tilde{g}^{ab} and ϕ generates the field equations

$$\tilde{\mathcal{R}}_{ab} - \frac{1}{2} \tilde{g}_{ab} \tilde{\mathcal{R}} = \frac{\kappa \tilde{T}_{ab}}{\phi} - \frac{3}{2\phi^2} \left(\tilde{\nabla}_a \phi \tilde{\nabla}_b \phi - \frac{1}{2} \tilde{g}_{ab} \tilde{\nabla}_c \phi \tilde{\nabla}^c \phi \right) + \frac{1}{\phi} \left(\tilde{\nabla}_a \tilde{\nabla}_b \phi - \tilde{g}_{ab} \tilde{\square} \phi \right) - \frac{V}{2\phi} \tilde{g}_{ab}, \tag{11}$$

$$\tilde{\square} \phi = \frac{\phi}{3} \left(\tilde{\mathcal{R}} - \frac{dV}{d\phi} \right) + \frac{1}{2\phi} \tilde{g}^{cd} \tilde{\nabla}_c \phi \tilde{\nabla}_d \phi. \tag{12}$$

³ See, however, refs. [71–77] exploring it.

The tilded energy-momentum tensor \tilde{T}_{ab} in (11) is related to the original energy-momentum tensor T_{ab} by $\tilde{T}_{ab} = \phi T_{ab}$. In other words, what appears on the right-hand side of the equations is κT_{ab} , *i.e.*, the original energy-momentum tensor of the sources.

The field equations (11) can be interpreted as usual Einstein field equations, but with an additional effective-matter source. In this context, notice the important fact, to which we shall come back below, that the absence of a radial matter flow in the original spacetime, $T_{01} = 0$, does not prevent such a radial flow from emerging in the new frame even with a conformal factor which depends only on time. This general pattern stems from the fact that the $(0, 1)$ component of the second derivative $\tilde{\nabla}_a \tilde{\nabla}_b \phi$ is not zero. Physically, this could be understood as the result of the original radial dependence of the metric transformed into an effective radial flow due to the stretching of spacetime in a time-dependent way. This is illustrated by the expression (35) of the energy flux density q_a , which would identically vanish only for a time-independent conformal factor.

In general, just as there is an induced energy flow in the form of a non-vanishing $T_{01}^{(\Omega)}$, the field equations for the matter fields ψ also acquire extra terms due to the new form of the matter Lagrangian, which picks up an explicit dependence on the scalar field ϕ . This fact does not, however, arise for conformally invariant matter fields, as is the case for the Maxwell field whose Lagrangian density $-\sqrt{-g} F_{ab} F^{ab}/4$ is invariant under conformal transformations. As such, the Maxwell equations in vacuo are also conformally invariant. We shall come back to this observation in sect. 4, where we examine the charged Thakurta black hole.

Now, Brans-Dicke theory with the particular value $-3/2$ of the ω -parameter is known to be pathological: the Brans-Dicke scalar ϕ (corresponding approximately to the inverse of the gravitational coupling) is not dynamical. In fact, by taking the trace of eq. (11),

$$\tilde{\mathcal{R}} = -\frac{\kappa \tilde{T}}{\phi} - \frac{3}{2\phi^2} \tilde{g}^{ab} \tilde{\nabla}_a \phi \tilde{\nabla}_b \phi + \frac{3\tilde{\square}\phi}{\phi} + \frac{2V}{\phi}, \tag{13}$$

and substituting it into eq. (12) reduces the latter to $\tilde{T} = 0$, and therefore $T = 0$, which is identically satisfied with a conformally invariant form of matter in the original frame and, in particular, (electro)vacuum. The usual Brans-Dicke dynamical equation for ϕ is thus completely lost and this field is not even subject to a first order constraint, becoming completely arbitrary. Correspondingly, the Cauchy problem for $\omega = -3/2$ is ill-posed ([79], see also [80–88]). This feature resurfaced recently in the literature with the revival of Palatini $f(\mathcal{R})$ gravity as an alternative to dark energy to explain the current acceleration of the universe, because this theory is equivalent to $\omega = -3/2$ Brans-Dicke gravity with a special potential [86–88].

These properties are not surprising because, while the geometry g_{ab} solves the Einstein equations (with no matter or with just the Maxwell field), the conformal factor Ω is completely arbitrary and is introduced *ad hoc* without being required to satisfy any rule or physical equation. Requiring Ω to coincide with the scale factor of a “background” FLRW universe does introduce some physics into this picture, but this is still an artificial way to force a geometry to do what we want. While the goal of the transformation (2) is to generate new solutions \tilde{g}_{ab} of GR with some desired properties, these can always be seen also as solutions of the (pathological) $\omega = -3/2$ Brans-Dicke gravity, possibly with a mass potential.

3 Relations between conformal GR solutions

Being concerned here specifically with the non-rotating Thakurta cosmological black hole, we discuss in this section an ambiguity present in the literature about such a black hole and the Sultana-Dyer one, which is also obtained by conformally transforming the same GR seed geometry.

Let the metric g_{ab} be an (electro)vacuum solution of the Einstein equations which can be expressed in various coordinate systems. Let $g_{\mu\nu}$ and $g_{\mu'\nu'}$ denote, respectively, the metric components in two coordinate systems (for example, consider the Schwarzschild metric in Schwarzschild, isotropic, Kerr-Schild, or Eddington-Finkelstein coordinates [89]). By conformally transforming g_{ab} with a conformal factor Ω , one obtains the two expressions $\tilde{g}_{\mu\nu} = \Omega^2 g_{\mu\nu}$ and $\tilde{g}_{\mu'\nu'} = \Omega^2 g_{\mu'\nu'}$ of the same metric. This stems from the one-to-one character of the conformal transformations (2) in the case of (electro)vacuum, as shown in ref. [59]. There are, however, incorrect claims to the contrary in the literature. For example, in ref. [42], the Schwarzschild metric in Schwarzschild coordinates (t, r, θ, ϕ) and in isotropic coordinates (t, ρ, θ, ϕ) , respectively,

$$ds_{(S)}^2 = -\left(1 - \frac{2m}{r}\right) dt^2 + \frac{dr^2}{1 - \frac{2m}{r}} + r^2 d\Omega_{(2)}^2, \tag{14}$$

$$= -\left(\frac{1 - \frac{m}{2\rho}}{1 + \frac{m}{2\rho}}\right)^2 dt^2 + \left(1 + \frac{m}{2\rho}\right)^4 \left(d\rho^2 + \rho^2 d\Omega_{(2)}^2\right), \tag{15}$$

(where $d\Omega_{(2)}^2 = d\theta^2 + \sin^2\theta d\varphi^2$ is the line element on the unit 2-sphere) is conformally transformed. If the line element in the form (14) is used, one obtains the non-rotating Thakurta metric

$$ds_{(T)}^2 = a^2(t) \left[- \left(1 - \frac{2m}{r} \right) dt^2 + \frac{dr^2}{1 - \frac{2m}{r}} + r^2 d\Omega_{(2)}^2 \right], \quad (16)$$

where $a(t)$ is the scale factor of the FLRW “background” universe into which the Schwarzschild black hole gets embedded. In ref. [42], the line element

$$ds^2 = a^2(t) \left[- \left(\frac{1 - \frac{m}{2\rho}}{1 + \frac{m}{2\rho}} \right)^2 dt^2 + \left(1 + \frac{m}{2\rho} \right)^4 \left(d\rho^2 + \rho^2 d\Omega_{(2)}^2 \right) \right] \quad (17)$$

obtained by conformally transforming the Schwarzschild line element in its form (15) with the same conformal factor a , is presented as a new GR solution alternative to the Thakurta one. However, the usual coordinate transformation

$$\rho \rightarrow r = \rho \left(1 + \frac{m}{2\rho} \right)^2 \quad (18)$$

turns the line element (17) into (16).

In contrast with the two forms (16) and (17), the non-rotating Thakurta and the Sultana-Dyer [41] solutions are genuinely different from each other, in spite of being both conformal to Schwarzschild because they are generated using two different conformal factors in eq. (2). This fact (remarked in ref. [44]) is not obvious in the coordinate systems normally used in the literature. The Sultana-Dyer line element is [41]

$$\begin{aligned} ds_{(SD)}^2 &= a^2(\tau) \left[-d\tau^2 + \frac{2m}{r} (d\tau + dr)^2 + dr^2 + r^2 d\Omega_{(2)}^2 \right] \\ &= a^2(\tau) \left[- \left(1 - \frac{2m}{r} \right) d\tau^2 + \frac{4m}{r} d\tau dr + \left(1 + \frac{2m}{r} \right) dr^2 + r^2 d\Omega_{(2)}^2 \right], \end{aligned} \quad (19)$$

where $a(\tau) = \tau^2$ and $m > 0$ is the mass of the original Schwarzschild black hole [41]. It is already clear from this last expression of the Sultana-Dyer metric that the latter is fundamentally different from the conformal Schwarzschild metric (16) that has a conformal factor depending only on time. To make this difference more apparent, let us introduce a new time coordinate t defined by

$$\tau(t, r) = t + 2m \ln \left| \frac{r}{2m} - 1 \right|, \quad (20)$$

which will be interpreted as the conformal time of the FLRW “background” universe. Differentiation gives

$$d\tau = dt + \frac{2m dr}{r(1 - 2m/r)}, \quad (21)$$

and substitution into eq. (19) turns this line element into the diagonal form

$$ds^2 = a^2(t, r) \left[- \left(1 - \frac{2m}{r} \right) dt^2 + \frac{dr^2}{1 - \frac{2m}{r}} + r^2 d\Omega_{(2)}^2 \right]. \quad (22)$$

In these coordinates, the Sultana-Dyer line element is explicitly conformal to Schwarzschild, with conformal factor

$$\Omega = a(t, r) = \tau^2(t, r) = \left(t + 2m \ln \left| \frac{r}{2m} - 1 \right| \right)^2, \quad (23)$$

which is clearly different from the conformal factor of the non-rotating Thakurta metric (16), which depends only on time. It is specifically this latter metric that is going to serve our purpose here. In the next section, we are first going to expose the construction and the physical features of the non-charged version in order to fully understand the more useful charged one, presented in sect. 4.2 and then used to examine the problem of the Cauchy horizon in sect. 4.3.

4 Thakurta geometry and strong cosmic censorship

4.1 Uncharged non-rotating Thakurta metric

The non-rotating Thakurta geometry has been the subject of recent attention [42, 44, 61–67] and is related to other exact solutions, hence it deserves a better look. As we shall see below, the other expression of the Thakurta line element (17) looks superficially like that of the McVittie metric [90]:

$$ds^2 = - \left(\frac{1 - \frac{m}{2ar}}{1 + \frac{m}{2ar}} \right)^2 dt^2 + a^2(t) \left(1 + \frac{m}{2ar} \right)^4 \left(dr^2 + r^2 d\Omega_{(2)}^2 \right). \tag{24}$$

But, while the mass coefficient in the McVittie metric is $M = m/a(t)$ (with constant m), that of the line element (17) is strictly constant. The difference is crucial because, allowing M to be different from its McVittie form $m/a(t)$, implies that there is a (purely spatial) radial energy flux with density q^a described by an imperfect fluid term in the matter stress-energy tensor [91]

$$T_{ab}^{(fluid)} = (P + \rho)u_a u_b + P g_{ab} + q_a u_b + q_b u_a. \tag{25}$$

Therefore, instead of a McVittie metric, the non-rotating Thakurta solution is a *generalized McVittie* geometry of the class presented in ref. [91] and studied in refs. [92–95]. The McVittie form $M = m/a(t)$ of the mass parameter corresponds to the condition $G^0_1 = 0$ and, because of the Einstein equations, to vanishing radial energy flux T^0_1 (this is known as the “McVittie condition”). By relaxing the McVittie condition, a radial flux T^0_1 associated with an imperfect fluid appears. As remarked below eq. (12), we can now understand the origin of this emergent radial flow in the non-rotating Thakurta spacetime as being due to the non-vanishing second derivative $\tilde{\nabla}_0 \tilde{\nabla}_1 a(t)$ of the time-dependent conformal factor $a(t)$.

Contrary to other classes of solutions introduced to describe central objects embedded in cosmological spacetimes, in universes that expand forever or in phantom cosmologies that end in a Big Rip at a finite future, the generalized McVittie class has a late-time attractor [96], which is precisely the non-rotating Thakurta solution⁴. This geometry is also the limit to GR of a family of solutions of Brans-Dicke theory found in refs. [52, 53]. Furthermore, it is also a solution of cuscuton gravity (a special Hořava-Lifschitz theory [97, 98]) and of shape dynamics [99].

As follows from the discussion of sect. 1, being conformal to the Schwarzschild black hole, the Thakurta metric (16) represents a spacetime filled with an artificially created effective matter that might exhibit negative energy densities in certain spacetime regions. In addition, given that the inverse metric g^{ab} of the original Schwarzschild line element used to create such a spacetime is singular at the black hole horizon $r = 2m$, we expect that the non-rotating Thakurta spacetime (16) will also possess a singularity at that same coordinate location. In fact, the coordinate singularity becomes, as we shall see, a true spacetime singularity in the conformally mapped geometry.

Using the action (6) and defining an energy-momentum tensor for the matter part by eq. (25), we find that to satisfy the Einstein equations (1), the components of the four-velocity vector and the energy flux density should be, respectively,

$$u_a = \left(-a \sqrt{1 - \frac{2m}{r}}, 0, 0, 0 \right), \tag{26}$$

$$q_a = \left(0, \frac{-m\dot{a}}{4\pi a^2 r^2 \left(1 - \frac{2m}{r}\right)^{3/2}}, 0, 0 \right). \tag{27}$$

On the other hand, the required energy density and pressure of the artificial fluid are found to be, respectively,

$$\rho = \frac{3\dot{a}^2}{8\pi a^4 (1 - 2m/r)}, \tag{28}$$

$$P = \frac{\dot{a}^2 - 2a\ddot{a}}{8\pi a^4 (1 - 2m/r)}. \tag{29}$$

The Ricci scalar of the Thakurta metric (16), computed directly from eq. (4), is

$$\mathcal{R} = \frac{6(\dot{H} + H^2)}{a^2(1 - 2m/r)}. \tag{30}$$

⁴ In ref. [96], the late-time attractor was not recognized as a non-rotating Thakurta solution and was called “comoving mass” solution instead. Similarly, refs. [52, 53] does not identify the $\omega \rightarrow \infty$ limit of its class of Brans-Dicke spacetimes as the Thakurta solution.

As expected, the Ricci scalar is singular at $r = 2m$. This singularity translates into a singular fluid as both the energy density and pressure (28) and (29) diverge there as well.

All the previous results concerning the possibility of a negative energy density and a singular character of the fluid necessary for the creation of the non-rotating Thakurta spacetime remain valid in the case of a charged and/or rotating Thakurta spacetime. In what follows, we examine this case in detail.

4.2 Charged non-rotating Thakurta metric

The charged non-rotating Thakurta (CNRT) metric of a black hole of constant mass m and constant charge Q embedded in a cosmological background of scale factor $a(t)$ reads

$$ds_{(CNRT)}^2 = a^2(t) \left[-f(r)dt^2 + \frac{dr^2}{f(r)} + r^2 d\Omega_{(2)}^2 \right], \quad (31)$$

where

$$f(r) = 1 - \frac{2m}{r} + \frac{Q^2}{r^2}. \quad (32)$$

This metric being conformal to the RN metric, and given the conformal invariance of the electromagnetic field F_{ab} , the corresponding expression of the latter for this geometry is the same as the one of the RN spacetime $F_{ab} = \partial_a A_b - \partial_b A_a$, with four-potential

$$A_a = \left(-\frac{Q}{r}, 0, 0, 0 \right). \quad (33)$$

The energy-momentum tensor $T_{ab}^{(em)}$ of the electromagnetic field that appears on the right-hand side of (5) is then the same as the one sourcing the RN metric. However, as for the uncharged Thakurta metric (16), an imperfect fluid source of the form (25) is now needed in addition to the electromagnetic energy-momentum tensor, with a four-velocity u_a and an energy flux density q_a given by

$$u_a = \left(-a\sqrt{f(r)}, 0, 0, 0 \right), \quad (34)$$

$$q_a = \left(0, -\frac{\dot{a}(mr - Q^2)}{4\pi a^2 r^3 f(r)^{3/2}}, 0, 0 \right). \quad (35)$$

The energy density and pressure of such a fluid are

$$\rho(t, r) = \frac{3\dot{a}^2}{8\pi a^4 f(r)}, \quad (36)$$

$$P(t, r) = \frac{\dot{a}^2 - 2a\ddot{a}}{8\pi a^4 f(r)}. \quad (37)$$

The energy-momentum tensors of the electromagnetic field and of the imperfect fluid appearing on the right-hand side of the Einstein equations and responsible for sourcing the metric thus read

$$\begin{aligned} T_{00}^{(fluid)} &= \frac{3\dot{a}^2}{8\pi a^2}, & T_{00}^{(em)} &= \frac{Q^2 f(r)}{8\pi r^4}, \\ T_{11}^{(fluid)} &= \frac{\dot{a}^2 - 2a\ddot{a}}{8\pi a^2 f(r)^2}, & T_{11}^{(em)} &= -\frac{Q^2}{8\pi r^4 f(r)}, \\ T_{22}^{(fluid)} &= \frac{r^2(\dot{a}^2 - 2a\ddot{a})}{8\pi a^2 f(r)}, & T_{22}^{(em)} &= \frac{Q^2}{8\pi r^2}, \\ T_{33}^{(fluid)} &= T_{22}^{(fluid)} \sin^2 \theta, & T_{33}^{(em)} &= T_{22}^{(em)} \sin^2 \theta, \\ T_{01}^{(fluid)} &= \frac{\dot{a}(mr - Q^2)}{4\pi a r^3 f(r)}. \end{aligned} \quad (38)$$

The origin of this imperfect fluid is, again, the non-vanishing second derivative $\tilde{\nabla}_0 \tilde{\nabla}_1 a(t)$ of the time-dependent conformal factor $a(t)$. Also, as for the non-charged Thakurta metric (16), a spacetime singularity arises at $r = m \pm \sqrt{m^2 - Q^2}$, given that the Ricci scalar is

$$\mathcal{R} = \frac{6(\dot{H} + H^2)}{a^2 f(r)}. \quad (39)$$

Since the charged Thakurta metric (31) is conformal to the Reissner-Nordström metric, which solves the vacuum Maxwell equations $\nabla_a F^{ab} = 0$ and $\nabla_{[a} F_{bc]} = 0$, one is also guaranteed to satisfy the Maxwell equations. This can be understood from our discussion of sect. 2 about the conformal invariance of such equations. Physically, although there is an induced effective matter creation and flow, the latter is uncharged, as shown by the expressions (34), (35). Therefore, the Maxwell equations are preserved due to the absence of induced currents.

4.3 Cauchy horizon and charged Thakurta geometry

As is well known [89], the RN geometry has a Cauchy horizon nested inside an event horizon, with radii

$$r_{\pm} = m \pm \sqrt{m^2 - Q^2}; \tag{40}$$

these horizons are null surfaces [89]. Since the null structure is left unchanged by conformal transformations, one would expect these two null horizons to be mapped into null horizons of the CNRT geometry (31), but they are mapped into null spacetime singularities instead. In fact, the Ricci scalar of the metric (31) is given by (39) and it diverges⁵ at the would-be Cauchy and event horizons $r = r_{\pm}$. The main point here is that the Cauchy horizon of the RN black hole disappears by embedding it into a non-static FLRW universe. The conformal transformation from the RN to the CNRT black hole brings an improvement if $|Q| \leq m$. It is well known [89] that, at small radii, the RN geometry exhibits a negative energy, as measured by the Misner-Sharp-Hernandez mass. In spherical symmetry, the Misner-Sharp-Hernandez mass M_{MSH} contained in a sphere of areal radius R is [100, 101]

$$1 - \frac{2M_{MSH}}{R} = \nabla^c R \nabla_c R. \tag{41}$$

For the RN black hole, this quantity is

$$M_{MSH} = m - \frac{Q^2}{2r} \tag{42}$$

and it is negative for small radii $r < Q^2/(2m)$. The Misner-Sharp-Hernandez mass of the CNRT geometry is computed either directly or by using the transformation property under conformal transformations [102, 103]

$$\tilde{M}_{MSH} = \Omega M_{MSH} - \frac{R^3}{2\Omega} \nabla^c \Omega \nabla_c \Omega - R^2 \nabla^c \Omega \nabla_c R. \tag{43}$$

In either way, one obtains for CNRT

$$\tilde{M}_{MSH} = a \left(M_{MSH} + \frac{3aH^2 r^3}{2f} \right). \tag{44}$$

This quantity is non-negative in the entire physical range $r > r_+$ if $|Q| \leq m$. In fact, since for the RN black hole $M_{MSH} \geq 0$ when $r \geq m/2$, it follows that $\tilde{M}_{MSH} > 0$ for any $r > r_+$. In the supercritical case $|Q| > m$ in which the RN geometry contains a naked singularity, instead, \tilde{M}_{MSH} becomes arbitrarily negative at small radii (the physical range of values of the radial coordinate is now $r > 0$).

4.4 Apparent horizons

The areal radius of the CNRT geometry (31) is

$$R(t, r) = a(t)r, \tag{45}$$

and, as usual in spherical symmetry, the AH radii are located by the roots of the equation [100, 101, 104]

$$\nabla^c R \nabla_c R = 0. \tag{46}$$

Since $\nabla_c R = \dot{a}r\delta_{c0} + a\delta_{c1}$, this equation corresponds to

$$\nabla^c R \nabla_c R = \frac{1}{f} (f^2 - H^2 r^2) = 0, \tag{47}$$

⁵ This fact was noted in [43].

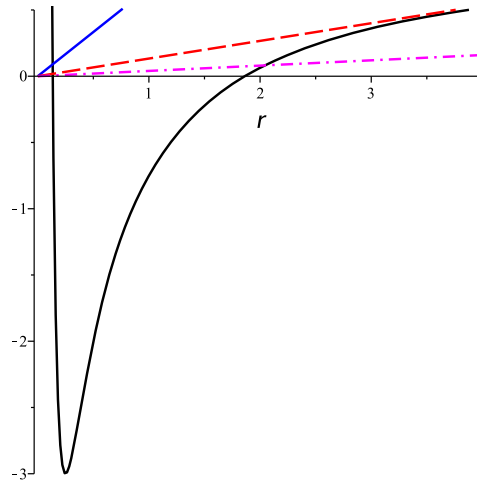


Fig. 1. The intersections between the curves $y = f(r)$ and $y = Hr$ corresponding to the AHs for $m > |Q|$. The solid, dashed, and dash-dotted straight lines correspond to progressively larger and larger times.

where $H \equiv \dot{a}/a$ is the Hubble parameter. Since $r > r_+$, we have $f > 0$ and, taking the positive sign in the square root of eq. (47), the AHs correspond to the roots of

$$f(r) \equiv 1 - \frac{2m}{r} + \frac{Q^2}{r^2} = Hr > 0, \tag{48}$$

therefore it is clear that the AHs (when they exist) do not coincide with the null spacetime singularities at r_{\pm} (which correspond to $f = 0$ instead). Equation (48) corresponds to the cubic

$$Hr^3 - r^2 + 2mr - Q^2 = 0, \tag{49}$$

but it is more interesting to discuss eq. (48) graphically. The AHs correspond to the intersections between the graph of the function $y = f(r)$ and the straight line $y = Hr$. A qualitative graphical analysis determines when roots exist and the number of these roots lying in the physical region $r > r_+$. Since

$$f'(r) = \frac{2}{r^2} \left(m - \frac{Q^2}{r} \right), \tag{50}$$

the function $f(r)$, which tends to $+\infty$ as $r \rightarrow 0^+$, decreases for $0 < r < r_{min}$, has a minimum $f_{min} = 1 - m^2/Q^2$ at $r_{min} = Q^2/m$, and it increases for $r > r_{min}$, asymptoting to 1 as $r \rightarrow +\infty$. For reference, we consider in all cases a FLRW universe which begins with a Big Bang at which the Hubble parameter H diverges and expands for an infinite time. For definiteness, we use a dust-dominated FLRW universe with scale factor $(t/t_0)^{2/3}$. Then, the slope $H(t)$ of the straight line through the origin $y = Hr$ decreases as time evolves, from positive infinity near the Big Bang to zero as $t \rightarrow +\infty$. We discuss separately the subcritical, critical, and supercritical situations $|Q| < m$, $|Q| = m$, and $|Q| > m$, respectively.

4.4.1 $|Q| < m$

When the CNRT metric is conformal to a subcritical RN black hole, the function $f(r)$ vanishes at $r_{\pm} = m \pm \sqrt{m^2 - Q^2}$ and its minimum $f_{min} = 1 - m^2/Q^2$ is negative. There are three possibilities, reported in fig. 1 (which is drawn for the parameter choice $|Q| = m/2$, $t_0 = 5m$).

The straight line $y = Hr$ intersects the curve $y = f(r)$ at only one point if the slope $H(t)$ is sufficiently large, that is, at early times near the Big Bang. This intersection corresponds to the unphysical region $r < r_-$ and there are no AHs.

As time goes by, the slope of the straight line $y = Hr$ decreases and the latter becomes tangent to the curve $y = f(r)$ at a critical time t_* , at which a pair of AHs is created. These AHs necessarily have a radius $r_* > r_+$, as is clear from fig. 1. This critical situation occurs when the slopes of the straight line and of the curve $f(r)$ coincide, $f'(r) = H(t)$, or

$$Hr^3 - 2mr + 2Q^2 = 0. \tag{51}$$

As time progresses ($t > t_*$) the two roots separate, becoming two distinct intersections between the two curves, which correspond to two distinct AHs of radii $r_{1,2}$ (labelled so that $r_2 > r_1$). As time grows and $t \rightarrow +\infty$, the line $y = Hr$

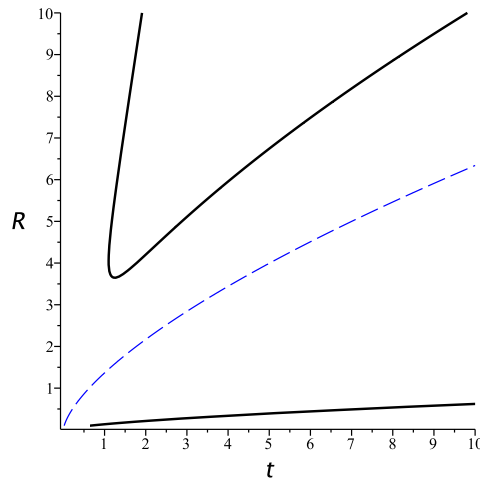


Fig. 2. The AHs areal radii as functions of the FLRW comoving time for $|Q| < m$ (“C-curve” phenomenology). The dashed line describes the null singularity at R_+ and the third AH below it is irrelevant for the spacetime corresponding to $r > r_+$.

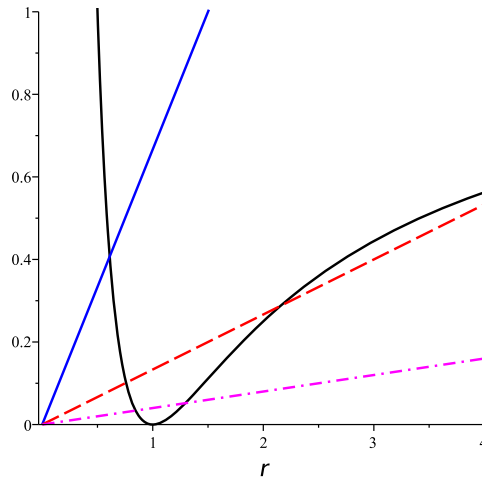


Fig. 3. The intersections between $y = f(r)$ and $y = Hr$ for $|Q| = m$. There are no AHs at early times (solid straight line), then a pair of AHs appears (dashed line). The cosmological one expands forever, while the black hole one shrinks and approaches the singularity at R_+ as $t \rightarrow +\infty$ (dash-dotted line).

becomes closer and closer to the horizontal and the smallest root $r_1 \rightarrow r_+$, while $r_2 \rightarrow +\infty$. The AH corresponding to the largest root r_2 is cosmological and r_2 reduces to the radius of the cosmological AH of the spatially flat FLRW universe $r_2 \approx 1/H$ (or $R_2 \approx a/H$) as $r_2 \rightarrow +\infty$, which happens as $t \rightarrow +\infty$. The smaller root r_1 corresponds to a black hole AH which always covers the null spacetime singularity ($r > r_+$) but approaches it as $t \rightarrow +\infty$. The behaviour of the areal radii of these AHs *versus* the comoving time of the “background” universe is given in fig. 2 for the parameters choice $|Q| = m/2, t_0 = 5m$. This phenomenology of AHs is well known and is dubbed “C-curve” in the literature [104].

4.4.2 $|Q| = m$

In this case the CNRT metric is conformal to an extremal RN black hole in which Cauchy and event horizons coincide. The null spacetime singularities of the CNRT geometry at $r_{\pm} = m$ coincide and there are only two spacetimes disconnected by it. Now, the function

$$f(r) = \left(1 - \frac{m}{r}\right)^2 \tag{52}$$

is non-negative and vanishes only at its minimum, achieved at $r_{\pm} = m$. Repeating the graphical analysis (see fig. 3), at early times and high values of H , there is only one root r_1 with $0 < r_1 < m$, which lies in the unphysical region, and there are no AHs. As time reaches a critical value t_* , two AHs appear, corresponding to a double root $r_* > m$ and to the straight line $y = Hr$ being tangent to the curve $y = f(r)$. At later times $t > t_*$, there are two distinct roots

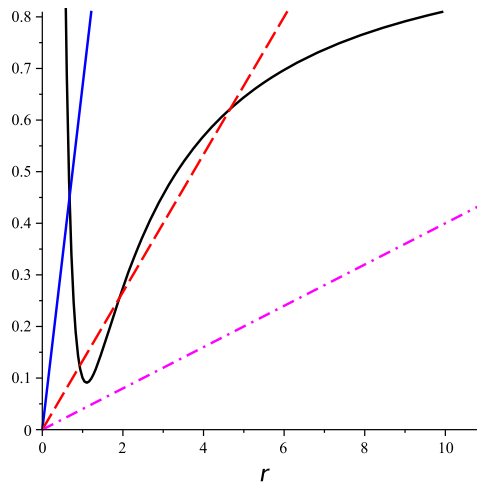


Fig. 4. The intersections between $y = f(r)$ and $y = Hr$ for $|Q| > m$. At early times (solid line) there is only one AH. As time progresses (dashed line), a pair of AHs appears and there are three of them. At later times a pair of AHs merge and disappear, leaving only a cosmological AH (dash-dotted line).

$r_{1,2}$ with $m < r_1 < r_2$. As the universe evolves and $t \rightarrow +\infty$, $r_1 \rightarrow m$ and $r_2 \rightarrow +\infty$. The AH at r_1 is interpreted as a black hole AH, while the one at radius r_2 is interpreted as a cosmological AH, which approaches the usual FLRW AH of areal radius $R_2 = a/H$ at late times. Qualitatively, the situation is similar to that of the previous case $|Q| < m$.

4.4.3 $|Q| > m$

In this case the CNRT geometry is conformal to a RN supercritical solution which does not have horizons and exhibits a naked singularity at $r = 0$. The physical range of the coordinate r is now the entire interval $r > 0$. The function $f(r)$ can be written as

$$f(r) = \frac{1}{r^2} [(r - m)^2 + Q^2 - m^2] \tag{53}$$

and is always positive, with positive minimum

$$f_{min} = f\left(\frac{Q^2}{m}\right) = 1 - \frac{m^2}{Q^2}. \tag{54}$$

The equation locating the AHs, $f(r) = Hr > 0$ can still be satisfied. Now the situation is qualitatively different from the previous cases.

Referring to fig. 4 for illustration, one sees that at early times, when the slope of the line $y = Hr$ is large, there is only one root (a cosmological AH) in the region $r < Q^2/m$: this spacetime region hosts a naked singularity. Later on, at a critical time t_1 , we have a single root $r_1 < Q^2/m$ and a double root $r_2 > Q^2/m$. As time progresses, this double root splits in two and there are three distinct AHs with radii $r_{1,2,3}$ satisfying

$$0 < r_1 < \frac{Q^2}{m} < r_2 < r_3. \tag{55}$$

As time progresses and the slope of the straight line decreases, r_1 increases and approaches Q^2/m , while r_2 decreases approaching Q^2/m , and r_3 increases without limit. At a critical time $t_2 > t_1$, r_1 and r_2 merge, corresponding to the annihilation of these two AHs, while r_3 (corresponding to a cosmological AH) still exists. At times $t > t_2$, there is only one intersection between $y = f(r)$ and $y = Hr$, with radius $r_3 \rightarrow +\infty$ as $t \rightarrow +\infty$. This surviving AH is a nearly-FLRW cosmological AH. At times $t > t_2$, the spacetime hosts a naked singularity not covered by a black hole AH. The behaviour of the areal radii of the AHs *versus* the comoving time of the “background” universe is given in fig. 5 for the parameter choice $|Q| = 3m/2$ and $t_0 = 5m$.

This behaviour of the AHs is the alternative to the “C-curve” phenomenology most often seen in the literature on AHs, and is called “S-curve” behaviour [104]. It was found for the first time in the Husain-Martinez-Nuñez solution of GR sourced by a free, canonical and minimally coupled scalar field [39]. The appearance of a naked singularity in the supercritical CNRT geometry is not too surprising, since the latter is conformal to a naked singularity spacetime. (This is also the case for the Husain-Martinez-Nuñez spacetime, which is conformal to the Fisher scalar field solution hosting a naked singularity [39].)

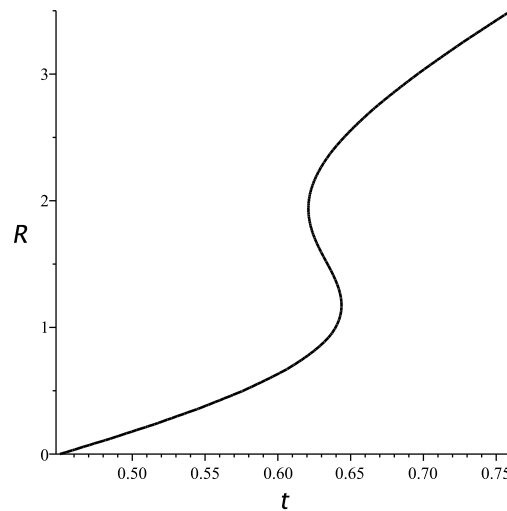


Fig. 5. The “S-curve” phenomenology of the AHs for $|Q| > m$. Initially there is only one AH, then a pair of AHs appears, one expanding and one shrinking. Later on, two AHs merge and disappear, leaving behind only a cosmological AH.

5 Cauchy horizon and McVittie metric

As discussed above, the central assumption made in refs. [2, 4] is a charged black hole embedded in a static de Sitter background, as well as a constant charge assigned to the black hole. While the weakness of the latter assumption will be dealt with elsewhere, our goal in this section is to deal with the former assumption using yet another spacetime representing a black hole embedded in a cosmological background. Indeed, we know from the Friedmann equation corresponding to an FLRW universe that, whenever there is matter, the universe cannot describe a de Sitter background as the Hubble parameter governed by such an equation can never be constant. Then, this fact allows one to argue that by embedding the RN black hole in a more “realistic” background, the Cauchy horizon would always be hidden behind a singularity. It turns out that this is what happens whenever the background is allowed to be non-static as is the case for the McVittie spacetime.

The McVittie spacetime (24) was introduced long ago in order to study the competition between cosmic expansion and local dynamics [90]. It is regarded as describing a black hole embedded in a FLRW universe and, recently, it has been the subject of considerable attention [42, 43, 91, 99, 105–116]. A charged version of the McVittie cosmological black hole was introduced in [117], generalized in [118], and further studied in [42, 43, 119–122]. The line element and Maxwell field assume the form

$$ds^2 = -\frac{[1 - \frac{(m^2 - Q^2)}{4a^2r^2}]^2}{[(1 + \frac{m}{2ar})^2 - \frac{Q^2}{4a^2r^2}]^2} dt^2 + a^2(t) \left[\left(1 + \frac{m}{2ar}\right)^2 - \frac{Q^2}{4a^2r^2} \right]^2 (dr^2 + r^2 d\Omega_{(2)}^2), \tag{56}$$

$$F^{01} = \frac{Q}{a^3r^2[1 - \frac{(m^2 - Q^2)}{4a^2r^2}][1 + \frac{m}{2ar}]^2 - \frac{Q^2}{4a^2r^2}}, \tag{57}$$

where the parameters $m > 0$ and Q describe the mass and the electric charge, respectively, while $a(t)$ is the scale factor of the “background” FLRW universe. The line element (56) interpolates between the RN spacetime (obtained for $a \equiv 1$) and the spatially flat FLRW metric (obtained for large values of r). The geometry reduces to the spatially flat FLRW one if $m = Q = 0$.

The AHs of the charged McVittie metric have been studied in [43, 122]. The areal radius is

$$R(t, r) = m + a(t)r + \frac{m^2 - Q^2}{4a(t)r}, \tag{58}$$

with $R \geq m$ if $|Q| \leq m$. The Ricci scalar

$$\mathcal{R} = 6 \left[2H^2 + \dot{H} \left(\frac{1 + \frac{m}{ar} + \frac{(m^2 - Q^2)}{4a^2r^2}}{1 - \frac{(m^2 - Q^2)}{4a^2r^2}} \right) \right] \tag{59}$$

(where $H(t) \equiv \dot{a}/a$) is singular at $R_* = m + \sqrt{m^2 - Q^2}$ if $|Q| \leq m$. This is the location of the outer apparent horizon of the RN geometry. This spacelike singularity splits the spacetime into two completely disconnected portions.

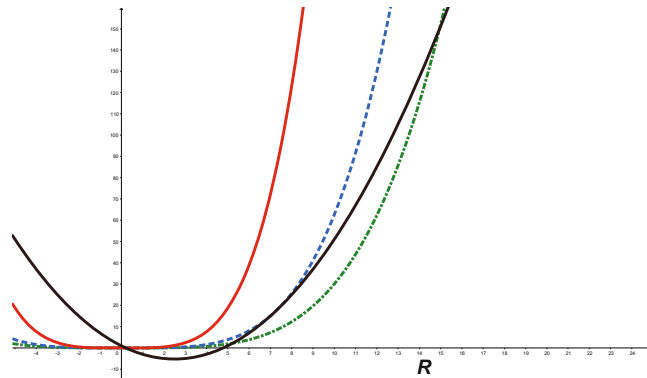


Fig. 6. The locations of the AHs for $|Q| > m$. Initially there is only one AH (intersection of the black solid curve $y = R^2 - 2mR + Q^2$ with the red curve $y = H^2 R^4$), then a pair of AHs appears (intersection of the black solid curve with the blue dashed curve $y = H^2 R^4$ with larger H at later times), then three AHs emerge (intersection of the black solid curve with the green dash-dotted curve $y = H^2 R^4$ at much later times).

The line element of the charged McVittie spacetime in (t, R, θ, ϕ) coordinates is

$$ds^2 = - \left(1 - \frac{2m}{R} + \frac{Q^2}{R^2} - H^2 R^2 \right) dt^2 - \frac{2HR dR dt}{\sqrt{1 - \frac{2m}{R} + \frac{Q^2}{R^2}}} + \frac{dR^2}{1 - \frac{2m}{R} + \frac{Q^2}{R^2}} + R^2 d\Omega^2. \tag{60}$$

Equation (46) locating the AHs becomes the quartic

$$\mathcal{G}(t, R) = H^2 R^4 - R^2 + 2mR - Q^2 = 0. \tag{61}$$

For large radii one obtains the asymptotic root $R \simeq H^{-1}$, which corresponds to the cosmological AH of the FLRW background. If $H \rightarrow 0$, there are only the two roots $R_{\pm} = m \pm \sqrt{m^2 - Q^2}$, where the smaller one, R_- , is always located inside the spherical singularity and R_+ lies outside of it. In order to locate the AHs numerically, one needs to fix the FLRW background. However, in order to have a general result, which would be independent of the particular conformal factor $a(t)$, we shall first repeat the procedure applied on the charged Thakurta metric in subsect. 4.4 and investigate the occurrence of a null internal horizon that we would identify with the Cauchy horizon. After locating these various AHs we shall investigate the possibility of identifying one of them —the internal one— as a Cauchy horizon.

The solutions to eq. (61) can be found graphically as shown in fig. 6 by detecting the intersections of the parabola $H^2 R^4$ (shown in red, blue, then green for consecutive times corresponding to smaller and smaller values of $H(t)$) with the parabola $R^2 - 2mR + Q^2$ (solid black curve). For different moments in the evolution of the universe described by the scale factor $a(t)$ we obtain the pattern shown in fig. 6.

In order for an AH detected by (61) to be null, its normal $\nabla_a \mathcal{G}$ needs to satisfy $\nabla_a \mathcal{G} \nabla^a \mathcal{G} = 0$. In terms of the metric, this reads

$$g^{RR} (\partial_R \mathcal{G})^2 + 2g^{Rt} \partial_R \mathcal{G} \partial_t \mathcal{G} + g^{tt} (\partial_t \mathcal{G})^2 = 0. \tag{62}$$

Because $\mathcal{G}(t, R) = 0$ at an AH, using (60) we can compute the needed components of the inverse metric:

$$g^{RR} = 0, \quad g^{Rt} = -1, \quad g^{tt} = -\frac{1}{H^2 R^2}. \tag{63}$$

On the other hand, computing the partial derivatives in (62), we find,

$$\partial_R \mathcal{G} = 4H^2 R^3 - 2R + 2m, \quad \partial_t \mathcal{G} = 2H \dot{H} R^4. \tag{64}$$

Substituting the results (63) and (64) in (62), we find the following condition for one of the AHs of the McVittie spacetime to be null:

$$H (4H^2 R^3 - 2R + 2m) + \dot{H} R^2 = 0. \tag{65}$$

Thus, we conclude that a given apparent horizon of the McVittie spacetime is not necessarily null. Instead, an algebraic equation in R and H has to be satisfied. One should keep in mind, though, the important fact that, because a Cauchy horizon is a null hypersurface, one needs two equations to be satisfied in order to be able to identify an AH with a Cauchy horizon. On one hand, for a given Hubble expansion rate H , eq. (61) gives for all times t the

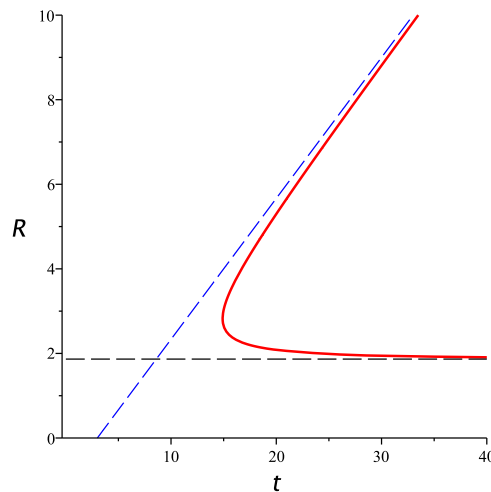


Fig. 7. The AH radii in the charged McVittie spacetime with FLRW scale factor $a(t) = a_0 t^3$. A black hole AH and a cosmological AH are born at a critical time. The cosmological horizon expands forever, while the black hole AH asymptotes to the spacetime singularity at $R_* = m + \sqrt{m^2 - Q^2}$ (the horizontal black dashed line). The (blue) dashed, oblique line of equation $R = H^{-1} - m$ is an asymptote for the cosmological AH at late times and large radii.

corresponding location R of the AH. On the other hand, eq. (65) is required for such a horizon to be null at whatever location it happens to be and at any corresponding time. However, satisfying both eqs. (61) and (65) can only happen at a finite number of instants of time t because extracting t in terms of R from the first and then substituting in the second leads to an algebraic equation in R alone and hence can only yield discrete pairs (t_0, R_0) .

These results show that, whenever the background is not static and not artificially created by a conformal transformation like in a McVittie spacetime, the would-be Cauchy horizon would only exist at certain instants of time. In the next subsection, we illustrate the occurrence of the various apparent horizons using a concrete model of an expanding universe.

5.1 AHs in a charged McVittie spacetime with scale factor $a(t) = a_0 t^p$

In keeping with the spirit of ref. [2], we choose a dark-energy dominated and accelerating FLRW “background” with scale factor $a(t) = a_0 t^p$ with $p > 0$ and, as a specific example, $p = 3$. The behaviour of the AH radii (in units of m) are plotted in figs. 7 and 8 as functions of the comoving time t (also measured in units of m) for the particular parameter choice $Q = \pm m/2$. (For ease of illustration, the scale is different in the two figures.)

Figure 7 reports the AH radii as given by (61) in the spacetime region $R > m + \sqrt{m^2 - Q^2}$ above the spacetime singularity. This is again a “C-curve” phenomenology. There are no AHs in this spacetime region at early times. Then, a black hole AH and a cosmological AH form as a pair at a critical time. The cosmological horizon expands forever, while the black hole horizon asymptotes to the spacetime singularity at $R = m + \sqrt{m^2 - Q^2}$ (represented by the black horizontal dashed line in fig. 7). The blue, dashed, oblique line of equation $R = H^{-1} - m$ is an asymptote for the cosmological AH at late times and large radii [122]. Once the two AHs form, there is no inner Cauchy horizon for the dynamical cosmological black hole thus formed. The singularity coincides with the outer event horizon of the RN black hole, which is obtained for $a = 1$. The third root of eq. (61) corresponds to an AH located in the other spacetime “below” the singularity $R < m + \sqrt{m^2 - Q^2}$. Figure 8 reports this third root of eq. (61). Since the two spacetime regions separated by the singularity are disconnected, this third AH has no implication, or meaning, for the region above the singularity. As remarked in ref. [122], embedding the RN black hole in a time-dependent cosmological “background” (not a locally static de Sitter one) has the effect of making the Cauchy horizon disappear. This fact is consistent with the known instability of this horizon in the RN spacetime [3].

The extremal case $|Q| = m$ can be discussed analytically. In this case the singularity is located at $R_* = m$ and eq. (61) for the AHs can be solved exactly, giving

$$R_{AH}^{(\pm)} = \frac{1 \pm \sqrt{1 - 4mH}}{2H}. \tag{66}$$

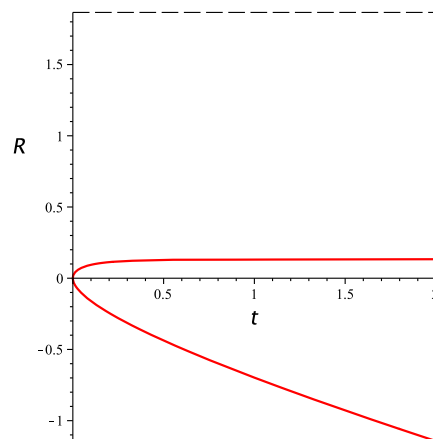


Fig. 8. The third AH is located in the region below the singularity (the dashed horizontal line) and does not belong to the region $R > R_*$. A fourth formal root of eq. (46) is negative and has no physical meaning.

In a universe with scale factor $a(t) = a_0 t^p$, the cosmological and black hole AHs $R_{AH}^{(+)}$ and $R_{AH}^{(-)}$ are created at the critical time $t_0 = 4pm$ and exist for all times $t > t_0$. Since $R > m_0$, for $t > t_0$ we have

$$m_0 < R_{AH}^{(-)} < R_{AH}^{(+)} < \frac{1}{H}. \quad (67)$$

Again, no inner black hole Cauchy horizon exists, speaking in favor of restoring determinism to GR.

6 Conclusions

We have investigated cosmological black holes obtained by conformally transforming either the neutral Schwarzschild black hole or the charged Reissner-Nordström black hole. The first case consists of the uncharged non-rotating Thakurta spacetime, while the second one consists of the charged version of this geometry. The general pattern emerging from obtaining conformal solutions by using “seed” solutions of the Einstein equations has been studied. The analysis shows that, while the resulting action after such a transformation is no longer an Einstein-Hilbert type action but a Brans-Dicke action with the pathological Brans-Dicke parameter $\omega = -3/2$, the resulting Brans-Dicke field equations may nevertheless be interpreted as effective Einstein field equations with an effective imperfect fluid playing the role of an additional source besides the electrovacuum associated with the seed [124, 125]. In fact, our whole procedure is based, not on any kind of Brans-Dicke theory, but rather on pure general relativity. The Brans-Dicke theory only suggests itself as the natural framework for interpreting the resulting action and equations of motion. Indeed, our approach, which consists in embedding a black hole in an expanding universe filled by fluids, takes its full meaning in Einstein’s gravity. The imperfect character of the induced effective fluid is manifested by the emergence of an energy flow and is unavoidable as long as the chosen embedding background is evolving, *i.e.*, the scale factor is time-dependent. This pattern is general and arises for both charged and uncharged black holes embedded in cosmological “backgrounds” obtained by this conformal technique. However, while an induced effective energy flow is automatically obtained even if it is absent in the original seed solution, no charged flow emerges even for charged black hole seeds, as a consequence of the conformal invariance of the vacuum Maxwell equations.

This technique has then been used to tackle the problem of determinism in GR by building the charged cosmological black hole in the form of the charged non-rotating Thakurta spacetime. Such a spacetime requires the presence of a neutral, but imperfect, fluid as a source. Nevertheless, the corresponding black hole is more realistic than the RNdS black hole as the former might be chosen to be embedded in a FLRW universe, in contrast to the latter which lives in a de Sitter “background”. We found that the Cauchy horizon of such a spacetime always hides, in the non-extremal case, behind a singularity.

The same analysis has been performed on another type of charged black hole embedded in a cosmological “background”, the McVittie geometry. We found that whenever the background is not static nor artificially created by a conformal transformation as in the case of the charged non-rotating Thakurta spacetime, the would-be Cauchy horizon appears only at certain instants of time. Hence, those locations could not really qualify as the loci of a real Cauchy horizon that would put determinism within GR in jeopardy. Indeed, Cauchy horizons are necessarily null hypersurfaces [15], whereas the would-be inner Cauchy horizon of McVittie spacetime is mainly a non-null AH, except at discrete instants of time.

Now, one might wonder whether the various theoretical models used here could be of any practical use in real cosmology, or are they just tools for investigating fundamental theoretical issues, such as the loss of determinism in GR. All three of the models presented here, the non-charged and the charged non-rotating Thakurta spacetimes, as well as the McVittie spacetime, are pure theoretical constructs intended for creating a physical setting that would be as close to the real systems of nature as possible. They satisfactorily take into account the fact that real black holes in nature represent inhomogeneities, with induced backreactions, in an otherwise smooth and homogeneous expanding universe. We cannot claim, however, that our models could have real astrophysical objects as counterparts in nature. The first two models, although based on the more “realistic” Schwarzschild black hole, cannot be used in real cosmology because they emerge from a pure theoretical technique. In fact, while the end product of such a technique is closer to the real black holes in our expanding universe, the byproduct that comes with such a construct is, as we saw, the presence of an artificial imperfect fluid. The third model is also a pure theoretical black hole which is, by construction, already embedded in an expanding universe. In contrast to the first two models, however, the third one is conceptually more attractive as it is free of any artificial fluids. Yet, the very absence of any kind of fluid around such a black hole prevents, in turn, the model from totally representing a realistic system of nature. Therefore, from this perspective the first two models become, precisely thanks to the presence of their imperfect fluids (although artificial) more “realistic”. For inhomogeneous exact solutions with perfect fluids, let alone those that lack fluids in their background, are of very limited use in astrophysics. In fact, heat fluxes and/or anisotropic stresses, supplied only by imperfect fluids, are needed in any kind of simulation and/or representation of realistic astrophysical objects in nature. The full merit of all three models is thus to investigate and test the formalism of GR in settings that are closer to the real world. This, indeed, helps greatly avoiding eventual traps coming from general conclusions—here concerning determinism in GR—based on models that are far from resembling our real expanding universe.

Now, the use of the charged McVittie spacetime (excluding the case in which it reduces to the RNdS space for $H = \text{const.}$) has of course conceptual weaknesses too. First, before the critical time at which the black hole/cosmological AH pair is created, there is a naked singularity and this solution of the Einstein equations cannot be obtained as the development of regular Cauchy data. Second, AHs ultimately depend on the foliation [17, 18], although all spherically symmetric foliations (the only ones of practical importance here) determine the same AHs [19]. Third, while the RN solution is the most general spherical and locally static electrovacuum solution of the Einstein equations with positive Λ , in the presence of a fluid there is no general solution and the charged Thakurta and McVittie geometries cannot claim such a degree of generality. In spite of these shortcomings, a time-dependent FLRW “background” is a more general setup for a charged black hole than the de Sitter one. Once (local) staticity is removed, there is no trace of inner Cauchy horizons in charged black holes, according to our models. This result agrees with the results of refs. [5–8] which restore determinism to Einstein theory. Given the importance of the issue, however, one still hopes that an experimental test, analogous to the one proposed in ref. [123] to test the Weak Cosmic Censorship Hypothesis, could also be devised to test the Strong Cosmic Censorship Hypothesis and bring a decisive conclusion about the fate of determinism in GR.

The authors are grateful to the anonymous referee for the pertinent remarks that helped improve the clarity of the manuscript. DKC thanks the Scientific and Technological Research Council of Turkey (TÜBİTAK) for a postdoctoral fellowship through the Programme BİDEB-2219 and Namık Kemal University for support. FH and VF are supported by the Natural Sciences and Engineering Research Council of Canada (Grants No. 2017-05388 and No. 2016-03803), and all authors thank Bishop’s University.

Publisher’s Note The EPJ Publishers remain neutral with regard to jurisdictional claims in published maps and institutional affiliations.

References

1. R. Penrose, *Singularities and Time Asymmetry*, in *General Relativity, an Einstein Centenary Survey*, edited by S.W. Hawking, W. Israel (Cambridge University Press, Cambridge, 1979).
2. V. Cardoso, J.L. Costa, K. Destounis, P. Hintz, A. Jansen, *Phys. Rev. Lett.* **120**, 031103 (2018).
3. E. Poisson, W. Israel, *Phys. Rev. D* **41**, 1796 (1990).
4. H. Reall, *Phys. Viewp.*, <https://doi.org/10.1103/Physics.11.6> (2018).
5. S. Hod, *Nucl. Phys. B* **941**, 636 (2019).
6. S. Hod, *Phys. Lett. B* **780**, 221 (2018).
7. M. Van de Moortel, arXiv:1804.04297 (2018).
8. O.J.C. Dias, F.C. Eperon, H.S. Reall, J.E. Santos, *Phys. Rev. D* **97**, 104060 (2018).
9. V. Prasad, R. Srinivasan, S. Gutti, *Phys. Rev. D* **99**, 024023 (2019).
10. M. Dafermos, Y. Shlapentokh-Rothman, *Class. Quantum Grav.* **35**, 195010 (2018).
11. O.J.C. Dias, H.S. Reall, J.E. Santos, *JHEP* **10**, 001 (2018).
12. Y. Mo, Y. Tian, B. Wang, H. Zhang, Z. Zhong, *Phys. Rev. D* **98**, 124025 (2018).
13. V. Cardoso, J.L. Costa, K. Destounis, P. Hintz, A. Jansen, *Phys. Rev. D* **98**, 104007 (2018).

14. L. Amendola, S. Tsujikawa, *Dark Energy, Theory and Observations* (Cambridge University Press, Cambridge, UK, 2010).
15. R.M. Wald, *General Relativity* (Chicago University Press, Chicago, 1984).
16. V. Faraoni, *Cosmology in Scalar Tensor Gravity Fundamental Theories of Physics Series*, Vol. **139** (Kluwer Academic, Dordrecht, 2004).
17. R.M. Wald, V. Iyer, Phys. Rev. D **44**, R3719 (1991).
18. E. Schnetter, B. Krishnan, Phys. Rev. D **73**, 021502 (2006).
19. V. Faraoni, G.F.R. Ellis, J.T. Firouzjaee, A. Helou, I. Musco, Phys. Rev. D **95**, 024008 (2017).
20. LIGO Scientific Collaboration and Virgo Collaboration (B.P. Abbott *et al.*), Phys. Rev. Lett. **116**, 061102 (2016).
21. LIGO Scientific Collaboration and Virgo Collaboration (B.P. Abbott *et al.*), Phys. Rev. X **6**, 041015 (2016).
22. LIGO Scientific Collaboration and Virgo Collaboration (B.P. Abbott *et al.*), Phys. Rev. Lett. **116**, 241103 (2016).
23. LIGO Scientific Collaboration and Virgo Collaboration (B.P. Abbott *et al.*), Phys. Rev. Lett. **118**, 221101 (2017).
24. R.H. Dicke, Phys. Rev. **125**, 2163 (1962).
25. Y. Fujii, K. Maeda, *The Scalar-Tensor Theory of Gravitation* (Cambridge University Press, Cambridge, UK, 2003).
26. F. Hammad, Int. J. Mod. Phys. D **25**, 1650081 (2016).
27. F. Hammad, Class. Quantum Grav. **33**, 235016 (2016).
28. F. Hammad, É. Massé, P. Labelle, Phys. Rev. D **98**, 104049 (2018).
29. F. Hammad, D. Dijamco, Phys. Rev. D **99**, 084016 (2019).
30. F. Hammad, É. Massé, P. Labelle, Phys. Rev. D **98**, 124010 (2018).
31. P. Szekeres, Proc. R. Soc. A **274**, 206 (1963).
32. S.N.G. Thakurta, Indian J. Phys. **55B**, 304 (1981).
33. N. van den Bergh, J. Math. Phys. **27**, 1076 (1986).
34. N. van den Bergh, Gen. Relativ. Gravit. **18**, 649 (1986).
35. J. Carot, L. Mas, J. Math. Phys. **27**, 2336 (1986).
36. N. van den Bergh, J. Math. Phys. **29**, 1451 (1988).
37. B.O.J. Tupper, J. Math. Phys. **31**, 1704 (1990).
38. J. Castejon-Amenedo, A.A. Coley, Class. Quantum Grav. **9**, 2203 (1992).
39. V. Husain, E.A. Martinez, D. Nuñez, Phys. Rev. D **50**, 3783 (1994).
40. O.A. Fonarev, Class. Quantum Grav. **12**, 1739 (1995).
41. J. Sultana, C.C. Dyer, Gen. Relativ. Gravit. **37**, 1349 (2005).
42. M.L. McClure, C.C. Dyer, Class. Quantum Grav. **23**, 1971 (2006).
43. M.G. Rodrigues, V.T. Zanchin, Class. Quantum Grav. **32**, 115004 (2015).
44. M.M.C. Mello, A. Maciel, V.T. Zanchin, Phys. Rev. D **95**, 084031 (2017).
45. J. Loranger, K. Lake, Phys. Rev. D **78**, 127501 (2008).
46. H. Moradpour, A. Dehghani, M.T. Mohammadi Sabet, Mod. Phys. Lett. A **30**, 1550207 (2015).
47. S. Hansraj, S.D. Maharaj, A.M. Msomi, K.S. Govinder, J. Phys. A **38**, 4419 (2005).
48. S. Hansraj, Gen. Relativ. Gravit. **44**, 125 (2012).
49. S. Hansraj, K.S. Govinder, N. Mewalal, J. Appl. Math. **2013**, 196385 (2013).
50. K. Bronnikov, Acta Phys. Pol. B **4**, 251 (1973).
51. J.D. Bekenstein, Ann. Phys. (NY) **82**, 535 (1974).
52. T. Clifton, D.F. Mota, J.D. Barrow, Mon. Not. R. Astron. Soc. **358**, 601 (2005).
53. V. Faraoni, A.F. Zambrano Moreno, Phys. Rev. D **86**, 084044 (2012).
54. J.P. Abreu, P. Crawford, J.P. Mimoso, Class. Quantum Grav. **11**, 1919 (1994).
55. A.Yu. Kamenshchik, E.O. Pozdeeva, A. Tronconi, G. Venturi, S.Yu. Vernov, Class. Quantum Grav. **31**, 105003 (2014).
56. S. Vignolo, S. Carloni, F. Vietri, Phys. Rev. D **88**, 023006 (2013).
57. V. Faraoni, S.D. Belknap-Keet, Phys. Rev. D **96**, 044040 (2017).
58. V. Faraoni, D.K. Çiftci, S.D. Belknap-Keet, Phys. Rev. D **97**, 064004 (2018).
59. V. Faraoni, F. Hammad, A.M. Cardini, T. Gobeil, Phys. Rev. D **97**, 084033 (2018).
60. J.L. Synge, *Relativity: The General Theory* (North Holland, Amsterdam, 1960).
61. H. Saida, T. Harada, H. Maeda, Class. Quantum Grav. **24**, 4711 (2007).
62. V. Faraoni, Phys. Rev. D **76**, 104042 (2007).
63. H. Culetu, J. Phys. Conf. Ser. **437**, 012005 (2013).
64. K. Bhattacharya, B.R. Majhi, Phys. Rev. D **94**, 024033 (2016).
65. B.R. Majhi, Phys. Rev. D **92**, 064026 (2015).
66. B.R. Majhi, JCAP **05**, 014 (2014).
67. A.B. Nielsen, J.T. Firouzjaee, Gen. Relativ. Gravit. **45**, 1815 (2013).
68. N. Deruelle, M. Sasaki, Springer Proc. Phys. **137**, 247 (2011).
69. V. Faraoni, A.B. Nielsen, Class. Quantum Grav. **28**, 175008 (2011).
70. A.B. Nielsen, J.T. Firouzjaee, Gen. Relativ. Gravit. **45**, 1815 (2013).
71. J.L. Anderson, Phys. Rev. D **3**, 1689 (1971).
72. J. O'Hanlon, B. Tupper, Nuovo Cimento B **7**, 305 (1972).
73. J. O'Hanlon, J. Phys. A **5**, 803 (1972).
74. S. Deser, Ann. Phys. (NY) **59**, 248 (1970).
75. G.A. Barber, arXiv:gr-qc/0302088 (2003).

76. A. Davidson, *Class. Quantum Grav.* **22**, 1119 (2005).
77. M.P. Dabrowski, T. Denkiewicz, D. Blaschke, *Ann. Phys. (Leipzig)* **16**, 237 (2007).
78. C.H. Brans, R.H. Dicke, *Phys. Rev.* **124**, 925 (1961).
79. M. Salgado, *Class. Quantum Grav.* **23**, 4719 (2006).
80. D.R. Noakes, *J. Math. Phys.* **24**, 1846 (1983).
81. P. Teyssandier, P. Tourrenc, *J. Math. Phys.* **24**, 2793 (1983).
82. J. Cocke, J.M. Cohen, *J. Math. Phys.* **9**, 971 (1968).
83. N. Lanahan-Tremblay, V. Faraoni, *Class. Quantum Grav.* **24**, 5667 (2007).
84. V. Faraoni, *Class. Quantum Grav.* **26**, 168002 (2009).
85. V. Faraoni, N. Lanahan-Tremblay, *Phys. Rev. D* **78**, 064017 (2008).
86. T.P. Sotiriou, V. Faraoni, *Rev. Mod. Phys.* **82**, 451 (2010).
87. A. De Felice, S. Tsujikawa, *Living Rev. Relativ.* **13**, 3 (2010).
88. S. Nojiri, S.D. Odintsov, *Phys. Repts.* **505**, 59 (2011).
89. E. Poisson, *A Relativist's Toolkit* (Cambridge University Press, Cambridge, 2004).
90. G.C. McVittie, *Mon. Not. R. Astron. Soc.* **93**, 325 (1933).
91. V. Faraoni, A. Jacques, *Phys. Rev. D* **76**, 063510 (2007).
92. D.C. Guariento, M. Fontanini, A.M. da Silva, E. Abdalla, *Phys. Rev. D* **86**, 124020 (2012).
93. A. Maciel, D.C. Guariento, C. Molina, *Phys. Rev. D* **91**, 084043 (2015).
94. C. Gao, X. Chen, V. Faraoni, Y.-G. Shen, *Phys. Rev. D* **78**, 024008 (2008).
95. N. Afshordi, M. Fontanini, D.C. Guariento, *Phys. Rev. D* **90**, 084012 (2014).
96. V. Faraoni, C. Gao, X. Chen, Y.-G. Shen, *Phys. Lett. B* **671**, 7 (2009).
97. N. Afshordi, D.J.H. Chung, M. Doran, G. Geshnizjani, *Phys. Rev. D* **75**, 123509 (2007).
98. N. Afshordi, *Phys. Rev. D* **80**, 081502 (2009).
99. E. Abdalla, N. Afshordi, M. Fontanini, D.C. Guariento, E. Papantonopoulos, *Phys. Rev. D* **89**, 104018 (2014).
100. C.W. Misner, D.H. Sharp, *Phys. Rev.* **136**, B571 (1964).
101. W.C. Hernandez, C.W. Misner, *Astrophys. J.* **143**, 452 (1966).
102. V. Faraoni, V. Vitagliano, *Phys. Rev. D* **89**, 064015 (2014).
103. A. Prain, V. Vitagliano, V. Faraoni, M. Lapiere-Léonard, *Class. Quantum Grav.* **33**, 145008 (2016).
104. V. Faraoni, *Cosmological and Black Hole Apparent Horizons* (Springer, New York, 2015).
105. N. Afshordi, M. Fontanini, D.C. Guariento, *Phys. Rev. D* **90**, 084012 (2014).
106. V. Faraoni, A.F. Zambrano Moreno, R. Nandra, *Phys. Rev. D* **85**, 083526 (2012).
107. C. Gao, X. Chen, V. Faraoni, Y.-G. Shen, *Phys. Rev. D* **78**, 024008 (2008).
108. D.C. Guariento, F. Mercati, *Phys. Rev. D* **94**, 064023 (2016).
109. D.C. Guariento, J.E. Horvath, P.S. Custodio, J.A. de Freitas Pacheco, *Gen. Relativ. Gravit.* **40**, 1593 (2008).
110. N. Kaloper, M. Kleban, D. Martin, *Phys. Rev. D* **81**, 104044 (2010).
111. K. Lake, M. Abdelqader, *Phys. Rev. D* **84**, 044045 (2011).
112. P. Landry, M. Abdelqader, K. Lake, *Phys. Rev. D* **86**, 084002 (2010).
113. B.C. Nolan, *J. Math. Phys.* **34**, 178 (1993).
114. B.C. Nolan, *Phys. Rev. D* **58**, 064006 (1998).
115. B.C. Nolan, *Class. Quantum Grav.* **16**, 1227 (1999).
116. B.C. Nolan, *Class. Quantum Grav.* **16**, 3183 (1999).
117. Y.P. Shah, P.C. Vaidya, *Tensor* **19**, 191 (1968).
118. B. Mashhoon, M.H. Partovi, *Phys. Rev. D* **20**, 2455 (1979).
119. C.J. Gao, S.N. Zhang, *Phys. Lett. B* **595**, 28 (2004).
120. C.J. Gao, S.N. Zhang, *Gen. Relativ. Gravit.* **38**, 23 (2006).
121. V. Faraoni, A.F. Zambrano Moreno, *Phys. Rev. D* **88**, 044011 (2013).
122. V. Faraoni, A.F. Zambrano Moreno, A. Prain, *Phys. Rev. D* **89**, 103514 (2014).
123. K.S. Virbhadra, G.F.R. Ellis, *Phys. Rev. D* **65**, 103004 (2002).
124. L.O. Pimentel, *Class. Quantum Grav.* **6**, L263 (1989).
125. V. Faraoni, J. Côté, *Phys. Rev. D* **98**, 084019 (2018).